Journal of Physical and Theoretical Chemistry
of Islamic Azad University of Iran, 9 (3) 149-161: Fall 2012
(J. Phys. Theor. Chem. IAU Iran)
ISSN 1735-2126

Investigation of the Effect of Vanillin as a Green Corrosion Inhibitor for Stainless Steel Using Electrochemical Techniques

M. Shahidi*, E. Sasaei, M.Ganjehkaviri and M.R. Gholamhosseinzadeh

Department of Chemistry, Kerman Branch, Islamic Azad University, Kerman, Iran

Received March 2013; Accepted April 2013

ABSTRACT

Vanillin offers interesting possibilities for corrosion inhibition because of its safe use and high solubility in water. The effect of vanillin on the corrosion inhibition of AISI 304 stainless steel in 0.5M H_2SO_4 solution has been studied using potentiodynamic polarization and electrochemical impedance spectroscopy (EIS). Furthermore, this paper demonstrates that the electrochemical noise (EN) technique under open circuit conditions as the only truly noninvasive electrochemical method can be applied to investigate the corrosion inhibition. According to calculation of the total amount of noise charges due to all partial signals resulted from wavelet analysis of EN current data, it is possible to obtain the inhibition efficiency (IE) of an inhibitor. These IE values show a reasonable agreement with those obtained from potentiodynamic polarization and EIS measurements.

Keywords: Vanillin; Electrochemical noise; Wavelet Analysis; Inhibition Efficiency; Electrochemical Impedance

INTRODUCTION

Stainless steels play an important role in the modern world. Austenitic stainless steels represent more than 2/3 of the total stainless steel production [1]. Austenitic stainless steels are widely used materials because of their excellent corrosion resistance in various aggressive environments [2]. The corrosion inhibition of AISI 304 stainless steel in acidic media is a fundamental academic and industrial concern that has received a great deal of consideration [3, 4]. The most important fields of application are acid pickling, industrial acid cleaning, acid descaling, and oil well acidizing. Because of the general aggressiveness of acid solutions, inhibitors commonly are used to reduce the corrosion attack on metallic materials. The use of inhibitors is one of the most practical methods for protection against corrosion. However, the development of the novel corrosion inhibitors of natural source and non-toxic type has been considered to be more important and desirable. Vanillin, 4-hydroxy-3-methoxy benzaldehyde (Scheme 1), offers

---

*Corresponding author: shahidi@iauk.ac.ir interesting possibilities for corrosion inhibition because of its safe use and high solubility in water [5, 6]. The potential usages of vanillin discussed in this research are in line with the recent trend of the environment-friendly or green concept.

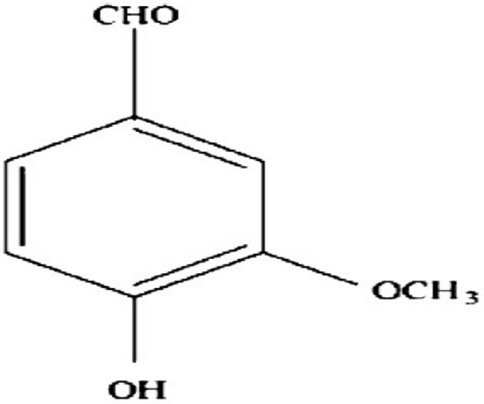

Scheme 1. The molecular structure of vanillin.

A very promising method for the investigation and monitoring of corrosion is the recording and analysis of the electrochemical noise (EN) data [7-11]. In contrast to other electrochemical methods for assessing corrosion, the measurement of EN offers the possibility to examine corrosion processes in real time with high sensitivity, which represents a very important advantage for the examination of the early stages of localized corrosion on passive alloys like stainless steels. EN measurements can be performed in freely corroding systems without the external application of electrical signals, so that the natural evolution of corrosion processes is assured. EN is defined as the fluctuations of potential or current originating from the localized events in a corrosion process. Two nominally identical working electrodes (WEs) are connected via a zero-resistance ammeter (ZRA) monitoring the coupling current between the electrodes.

To keep the measuring and data evaluation system as simple as possible, only current noise is measured in this study. In contrast to other ECN measuring systems no potential noise is measured. This avoids the use of reference electrodes which always present problems in long-term monitoring under service conditions due to fouling, potential drifts and degradation [10].

While the EN measurement is simple, understanding of the information included in the EN signals, the EN analysis, remains difficult. Wavelet transform (WT) is a mathematical tool that has gained popularity for EN analysis [12-17]. WT may be regarded as a variant of Fourier transform in which the continuous sine waves used in the Fourier transform are replaced by transient waves with a finite duration, known as wavelets. WT unlike Fourier transform can retain time domain information.

WT produces vectors of $d_1, d_2, ..., d_J$ and s_J termed ‘crystals’ which contain wavelet coefficients. The term ‘crystal’ is used because the wavelet coefficients in a crystal correspond to a set of translated wavelet functions arranged in a regular lattice [13]. The wavelet coefficients measure the similarity between the wavelet function and different segments of the signal. The wavelet coefficients in s_J are called smooth coefficients, while the remaining wavelet coefficients in $d_1, d_2, ..., d_J$ are called detail coefficients. Each crystal describes the original signal on a different scale.

The frequency range of each crystal is represented by the equation:

$$\left(f_1, f_2\right) = \left(2^{-j} f_s \ , \ 2^{1-j} f_s\right) \tag{1}$$

where f_s is sampling frequency, and j is the number of the crystal. The scale range of each crystal is given by the equation [14]:

$$(I_1, I_2) = \left(2^j \Delta t \ , \ 2^{j-1} \Delta t\right) \tag{2}$$

where Δt is the sampling interval $(\Delta t = 1/f_s)$. Table 1 shows the frequency and scale range of the case in which $J = 8$ and $f_s = 10Hz$.

Table 1. Frequency and Scale Range for $J = 8$ and $f_s = 10Hz$

Crystal name	Frequency range (Hz)	Scale range (s)
d1	10 - 5	0.1 – 0.2
d2	5 – 2.5	0.2 – 0.4
d3	2.5 – 1.25	0.4 – 0.8
d4	1.25 – 0.625	0.8 – 1.6
d5	0.625 – 0.312	1.6 – 3.2
d6	0.312 – 0.156	3.2 – 6.4
d7	0.156 – 0.0781	6.4 – 12.8
d8	0.0781 – 0.0391	12.8 – 25.6

The original signal can be reconstructed by adding the contributing wavelets weighted by their corresponding coefficients [13]. This process is known as inverse WT. If the inverse WT is limited to the coefficients of only one crystal rather than all crystals, it produces one smooth signal, PSs_J, and J detail signals, PSd_j. Each of these $J+1$ signals is called a partial signal (PS) [13, 15]. Each PS is a signal that it resembles the fluctuations of the original signal at a particular interval of frequency [15,16]. For example $PSd5$ represents all fluctuations of the original signal between $0.625 - 0.312Hz$, if the sampling frequency is equal to 10Hz. The unit of PS is the same as the EN signal one.

A coulombs counting method, namely CoulCount, has been developed as a means of studying localized corrosion [9, 10]. The total amount of noise charges exchanged between two WEs in a given time interval is collected (counted). It takes two steps from the digital current noise signals to the calculation of the time-related amount of noise charges: 1) elimination of the DC part and 2) summation of the time-related current levels [9]. The DC part (the part of the signal with fluctuations <0.1 Hz) is eliminated with hardware filters. The total amount of noise charges Q(t) at the time t is calculated according to the following equation [10]:

$$Q(t) = \sum_{i=0}^{t/\Delta t} |I_i| \Delta t \tag{3}$$

The reduction of data is achieved by averaging absolute current noise data, $|I_i|$ (e.g. 600 data points for 1 min) and corresponding adjustment of Δt (1 min).

In this paper, the use of vanillin as green corrosion inhibitor of AISI 304 in 0.5M H_2SO_4 solution have been studied by potentiodynamic polarization, electrochemical impedance spectroscopy (EIS) and electrochemical noise methods. The partial signals resulted from wavelet analysis of EN current data, instead of the hardware filtered noise signal (with fluctuations >0.1 Hz), has been employed to calculate the total amount of noise charges.

EXPERIMENTAL

AISI 304 stainless steel samples were of the following composition (in wt%): 0.08% C max., 1.96% Mn, 0.43% Si, 0.02% S, 18.74% Cr, 8.2% Ni, and the remainder Fe. Potentiodynamic polarization, EIS and EN measurements have been used to study the corrosion behavior of AISI 304 stainless steel in 0.5M H_2SO_4 solution without and with doping by vanillin at different concentrations. Before performing experiments, the specimens were connected to a copper wire at one end sealed using resin, with the other end that exposed as the WEs surface. Then the working surface was polished by wet abrasive papers through 600-2500 grade, washed with distilled water, degreased with ethanol, finally dried in air.

Potentiodynamic polarization, EIS and EN experiments were conducted using Autolab 302N potentiostat with Nova 1.6 software. This equipment allows resolutions of 0.76 μV for voltage signals and 10 nA for current signals. Potentiodynamic polarization and EIS measurements were conducted in a conventional three-electrode cell. A platinum rod was used as the counter and a saturated (KCl) Ag/AgCl electrode as reference electrode. To obtain the stabilized open circuit potential (OCP), the samples were immersed for 30 min in the solution before EIS and potentiodynamic polarization measurements. Polarization curves were recorded at a scan rate of 1 mV/s and Nova software was used for determination of corrosion current densities and Polarization parameters. A sinusoidal potential perturbation of 10 mV versus OCP was used in the EIS measurements and a frequency range from 10 mHz to 100 kHz was employed and Nyquist plots of the impedance data were analyzed with Nova software.

Two WEs were facing each other vertically at a distance of about 3 cm in the EN experiments. The EN records were collected just after immersion time and during 30 minutes. Two nominally identical WEs with surface areas of 100 mm^2 were used. The entire cell was placed inside a Faraday cage to limit external electromagnetic interference. The sampling frequency for the electrochemical noise data was 10Hz. The surfaces of alloy were observed in a CamScan MV2300 scanning electron microscope (SEM). Noise data were analyzed with wavelet technique using the orthogonal Daubechies wavelets of the fourth order (db4). The necessary calculations for construction of the SDPS plots were performed using Matlab software.

RESULTS AND DISCUSSION

Potentiodynamic polarization

Fig. 1 shows the potentiodynamic polarization curves of stainless steel in 0.5M H_2SO_4 solution in the absence and presence of vanillin. The relevant parameter values are listed in Table 2 (corrosion potential (E_{corr}), corrosion current density (i_{corr}), anodic Tafel slope (b_a) and cathodic Tafel slope (b_c)). It is clear that corrosion current density decreases as the concentration of inhibitor increases. Addition of vanillin to acid media affects both cathodic and anodic branches of the potentiodynamic polarization curves; therefore, vanillin behaves as mixed inhibitor. However, small potential shifts in the positive direction in the presence of inhibitor indicate that the effect of vanillin on the anodic reaction is more observable than on the cathodic reaction.

Table 2 presents values of the corrosion inhibition efficiency (IE) for which the expression in this case is:

$$IE\% = \frac{i_{corr} - i'_{corr}}{i_{corr}} \times 100 \qquad (4)$$

where i_{corr} and i'_{corr} are corrosion current densities in the uninhibited and inhibited cases, respectively. The IE values shows that this inhibition is more pronounced with increasing inhibitor concentration.

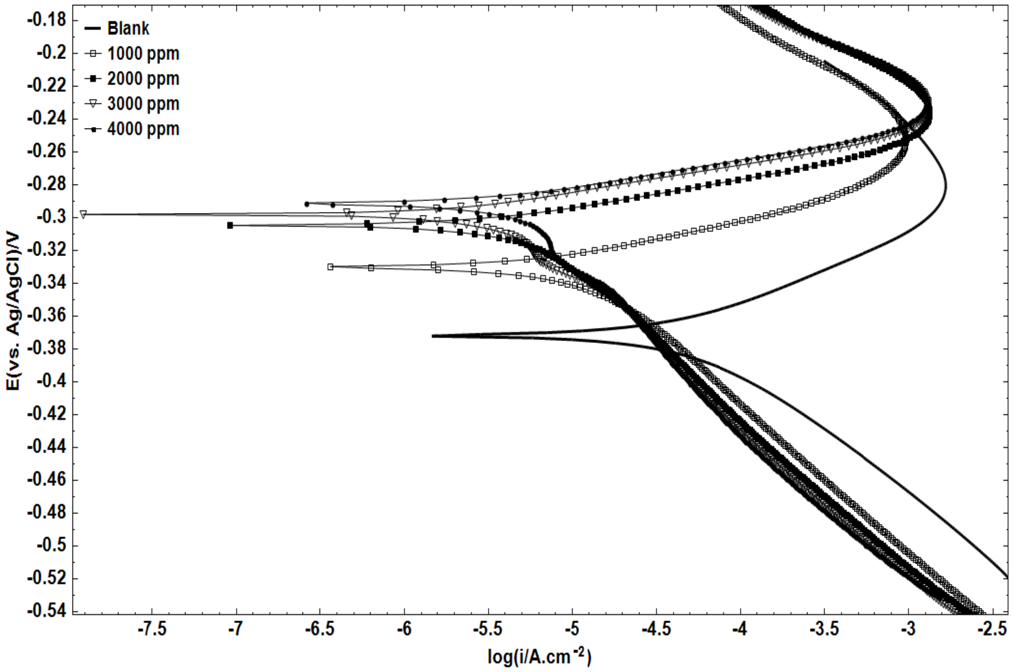

Fig. 1. Tafel polarization curves of stainless steel in 0.5M H_2SO_4 solution containing different concentrations of vanillin.

Table 2. Tafel Polarization Parameter Values for the Corrosion of Stainless Steel in 0.5M H_2SO_4 Solution Containing Different Vanillin Concentrations

C (ppm)	C (mM)	E_{corr}(vs.Ag/AgCl) (mV)	i_{corr} (μA.cm^{-2})	b_a (mV.dec^{-1})	b_c (mV.dec^{-1})	IE%
Blank	Blank	-372	54.9	75	51	-
1000	6.6	-330	11.6	89	29	79
2000	13.2	-304	5.3	18	98	90
3000	19.7	-298	3.4	16	93	94
4000	26.3	-291	2.7	17	91	95

To calculate the surface coverage, θ, it was assumed that the inhibition efficiency is mainly due to the blocking effect of the adsorbed species and hence θ=IE(%)/100 [18]. Here, it has been done an attempt for data fitting by Langmuir, Temkin and Frumkin isotherms (Fig. 2). The Langmuir adsorption isotherm was found to fit well with the experimental data (Fig. 2a), which can be expressed as:

$$\theta = \frac{KC}{1+KC} \tag{5}$$

or:

$$\frac{C}{\theta} = C + \frac{1}{K} \tag{6}$$

where θ is the surface coverage, C is the inhibitor concentration and K is the adsorption equilibrium constant. Straight line were obtained when C/θ were plotted against C (Fig. 2a). The correlation coefficient is close to 1.0, confirming that the adsorption of vanillin obeys the Langmuir isotherm. This isotherm is based on the assumption that all the adsorption sites are equivalent and that the particle binding occurs independently from the nearby sites being occupied or unoccupied [19].

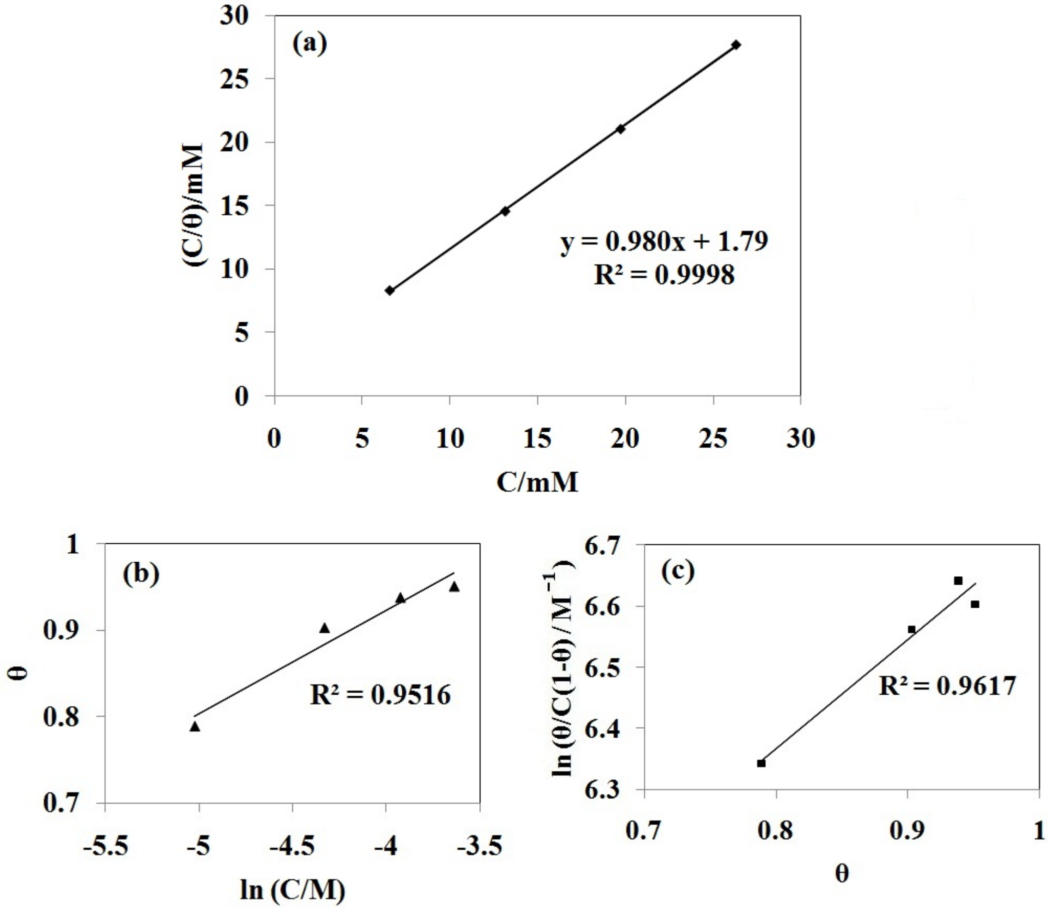

Fig. 2. Adsorption isotherms for stainless steel in 0.5M H_2SO_4 solution at the presence of different concentrations of vanillin from polarization data (a) Langmuir (b) Temkin and (c) Frumkin.

The relationship between the adsorption equilibrium constant and free energy of adsorption is given by:

$$K = \exp\left(\frac{-\Delta G^0_{ads}}{RT}\right) \qquad (7)$$

where R is the universal gas constant and T is the absolute temperature. A value for ΔG^0_{ads} equal to -15.7 kJ/mol can be calculated (as $K = 559 L.mol^{-1}$). A value of -20 kJ/mol is usually adopted as a threshold value between chemi- and physisorption [3]. Therefore, the calculated value for free energy of vanillin adsorption indicated that its adsorption on stainless steel had a physical character.

Vanillin is an aromatic aldehyde containing carbonyl, methoxy and hydroxyl groups arranged around the aromatic ring (Scheme 1). Thus, the adsorption of vanillin on the surface of stainless steel may take place through all these functional groups. The simultaneous adsorption of the three functional groups forces the vanillin molecule to be horizontally oriented at the surface of alloy [20]. As the inhibitor concentration increases, the area of the alloy surface covered by the inhibitor molecule also increases, leading to an increase in the IE [5].

Electrochemical impedance spectroscopy

Nyquist presentations of EIS for stainless steel in 0.5 M H_2SO_4 solution in the absence and presence of various concentrations of vanillin are shown in Fig. 3. In these spectra, variation of impedance response of stainless steel after addition of vanillin to the acid media is remarkable. Increasing the concentration of vanillin caused the values of charge transfer resistance shift to elevated amounts. Table 3 lists impedance parameters in the absence and presence of different concentrations of vanillin.

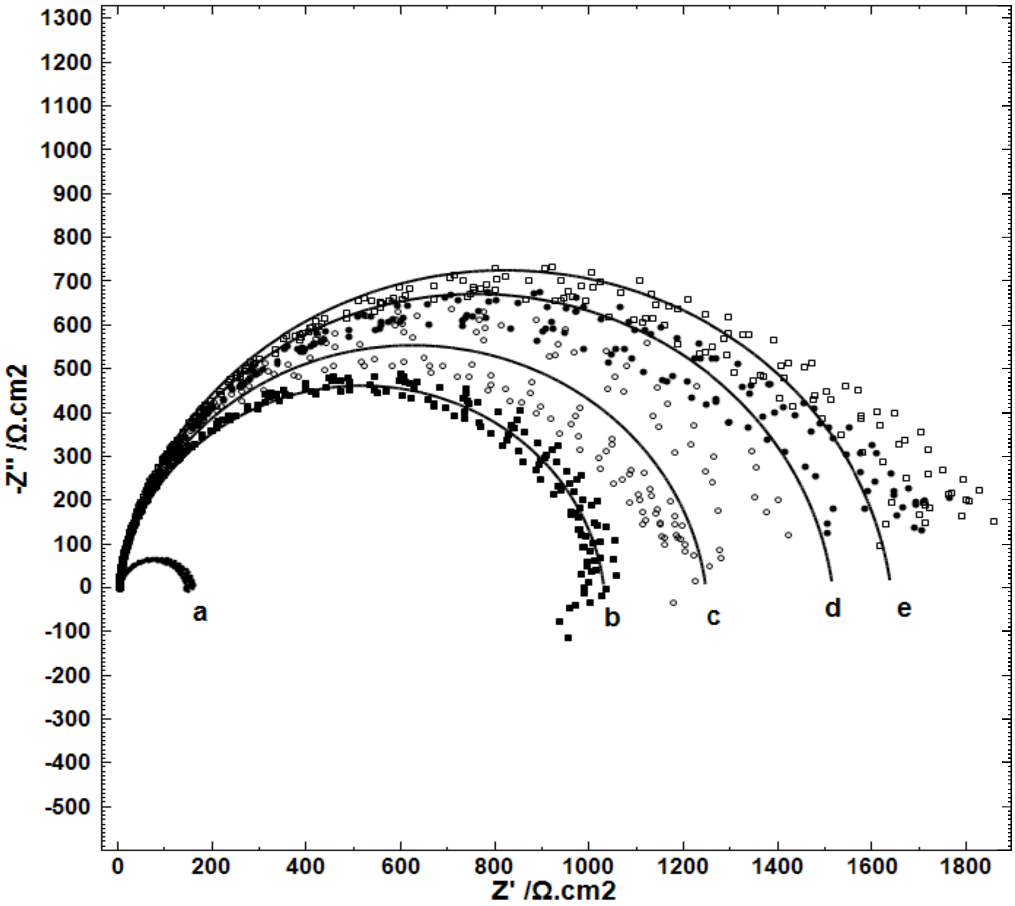

Fig. 3. Nyquist plots for stainless steel in 0.5M H_2SO_4 solution in the presence of the following vanillin concentrations (in ppm): (a) 0 (b) 1000 (c) 2000 (d) 3000 (e) 4000.

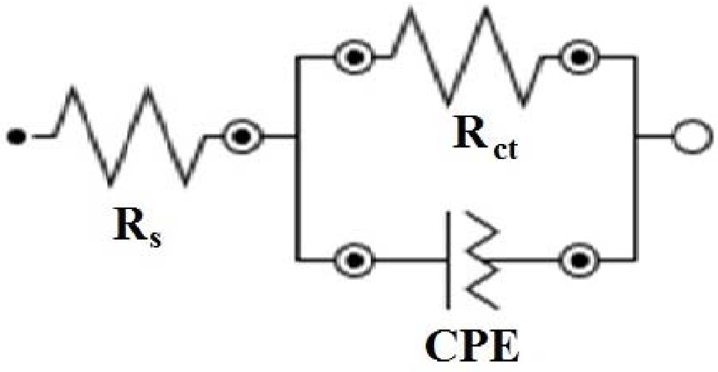

Scheme 2. The equivalent electrical circuit of the impedance spectra.

Scheme 2 shows the electrical equivalent circuit employed to analyze the impedance plots. In this scheme, R_s is the solution resistance and R_{ct} is the charge transfer resistance. The impedance of the constant phase element (CPE) is defined as follow [21]:

$$Z_{CPE} = \frac{1}{Y_0 \left(jw \right)^n} \tag{8}$$

where Y_0 is a proportional factor, j equals $\sqrt{-1}$, w is the angular frequency and n is the phase shift. For $n = 0$, Z_{CPE} represents a resistance with $R = Y_0^{-1}$, for $n = 1$ a capacitance with $C = Y_0$, for $n = 0.5$ a Warburg element and for $n = -1$ an inductive with $L = Y_0^{-1}$ [22]. Because it was observed (Table 3) that the phase shift was closely near 1, the CPE obeys the capacitive behavior.

Inhibition efficiencies in Table 3 were calculated through the following expression:

$$IE\% = \frac{R_{ct}^{'} - R_{ct}}{R_{ct}^{'}} \times 100 \tag{9}$$

where R_{ct} and $R_{ct}^{'}$ represent the charge transfer resistance, before and after addition of the inhibitor to the corrosion media, respectively. Comparison with the data in Table 2 shows satisfactory agreement with the inhibition efficiencies obtained from potentiodynamic polarization measurements.

Plots of the data for each isotherm showed the EIS data are agreed with the Langmuir isotherm (Fig. 4). Values of K and ΔG_{ads}^{0} in this case are 1389 $L.mol^{-1}$ and -17.9 $kJ.mol^{-1}$, respectively.

Electrochemical noise

The EN signals corresponding to two nominally identical WEs with 100 mm^2 surface area in the absence and presence of vanillin have been measured. Then the WT was employed to decompose each set of 18000 data points and the PSs of each signal were obtained.

Table 3. Impedance Parameter Values for the Corrosion of Stainless Steel in 0.5M H_2SO_4 Solution Containing Different Vanillin Concentrations

C (ppm)	R_s ($\Omega.cm^2$)	R_{ct} ($\Omega.cm^2$)	n	IE%
Blank	1.81	151	0.918	-
1000	1.94	1030	0.934	85
2000	1.95	1240	0.928	88
3000	1.97	1510	0.926	90
4000	1.86	1640	0.924	91

Table 4. EN Parameter Values Obtained on Stainless Steel in the Absence and Presence of Different Vanillin Concentrations

C (ppm)	Q_i (nCoul)								Q (nCoul)	IE%
	d1	d2	d3	d4	d5	d6	d7	d8		
Bln	1.7	2.6	5.1	14.6	49.8	224.5	977.6	4512.1	5787.9	-
1000	1.0	1.3	2.0	4.2	12.5	41.4	183.5	776.9	1022.8	82
2000	1.0	1.4	2.0	3.2	6.7	19.6	84.2	335.5	453.7	92
3000	0.9	1.3	1.9	3.1	6.3	18.6	66.8	171.1	270.1	95
4000	0.7	1.1	1.5	2.5	5.3	15.1	47.5	228.5	302.4	95

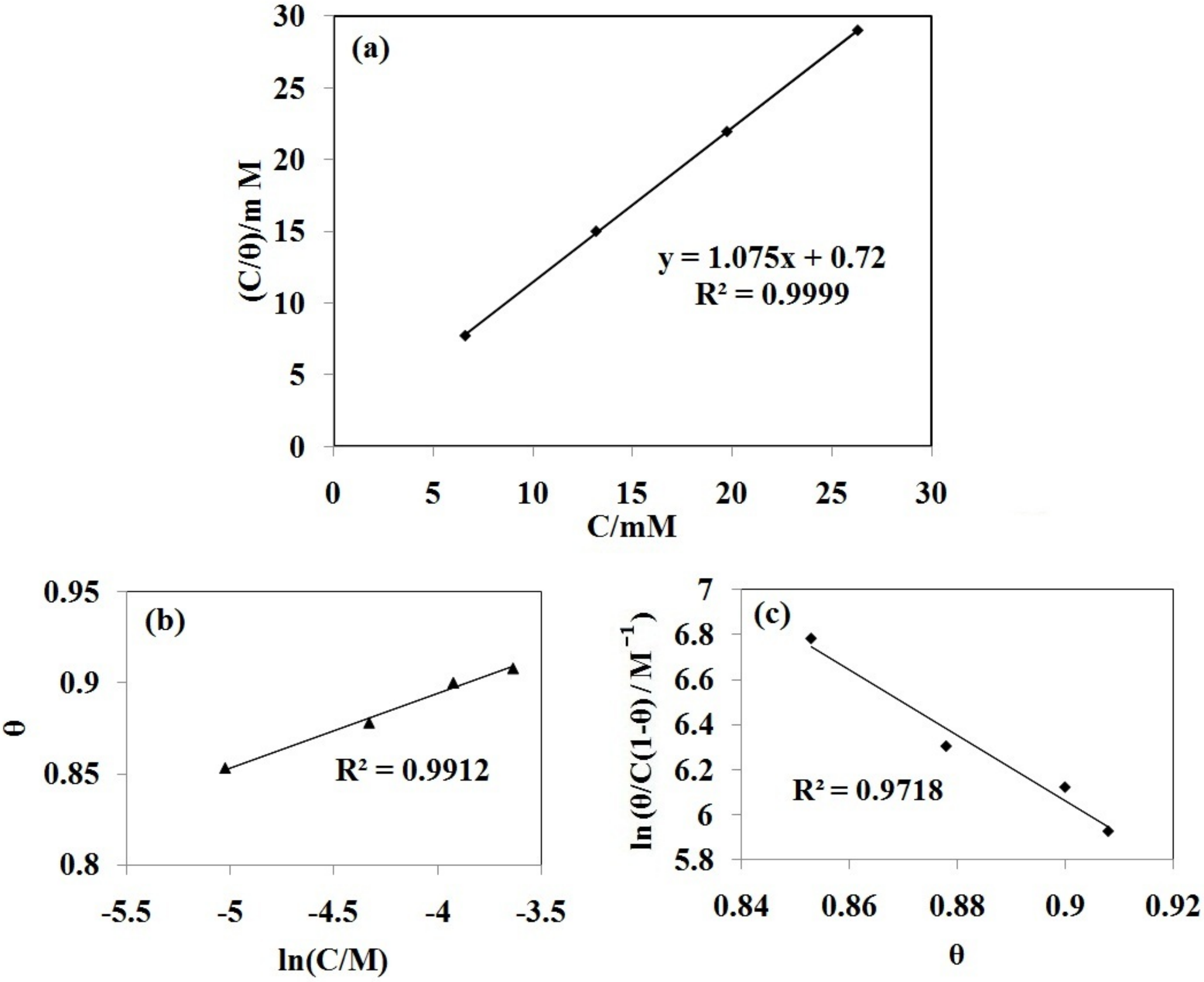

Fig. 4. Adsorption isotherms for stainless steel in 0.5M H_2SO_4 solution at the presence of different concentrations of vanillin from impedance data (a) Langmuir (b) Temkin and (c) Frumkin.

As mentioned above in the introduction, each PS is a signal which resembles the fluctuations of the original signal at a particular interval of frequency. Therefore, it is suitable to use the absolute mean of partial signal (AMPS) for calculation of the amount of noise charges at the particular interval of frequency. After calculation of the mean time width of each crystal, Δt, the amount of noise charges due to the ith PS, Q_i, can be computed. Fig. 5 shows the plot of Q_i vs. crystal name. The Q_i values can be summed to give the total amount of noise charges, Q (Table 4).

It seems suitable to define the corrosion inhibition efficiency as follow:

$$IE\% = \frac{Q - Q'}{Q} \times 100 \qquad (10)$$

where Q and Q' are the noise charges in the uninhibited and inhibited cases, respectively. Table 4 presents IE values obtained with EN measurements on stainless steel in different vanillin concentrations. Comparison with data in Tables 2 and 3 reveals that reasonable agreement is found with the IE values as obtained through potentiodynamic polarization and EIS measurements (Table 5).

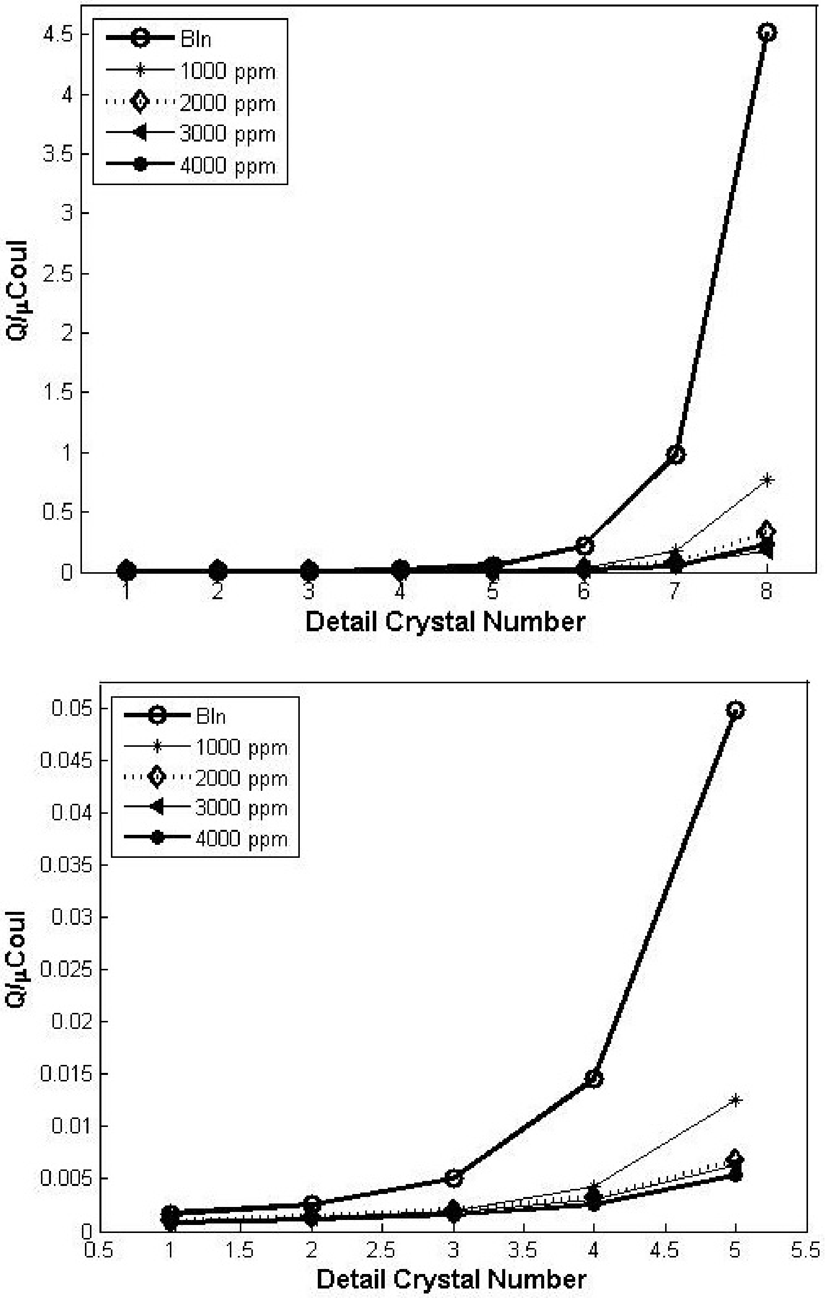

(a)

(b)

Fig. 5. (a) the plots and (b) the enlargement of the amount of noise charges resulted from each PS.

Table 5. Comparison of IE% Values Obtained on Stainless Steel from Three Electrochemical Techniques.

	IE%		
C (ppm)	**Tafel**	**EIS**	**EN**
1000	79	85	82
2000	90	88	92
3000	94	90	95
4000	95	91	95

Attempts were made to fit θ values to various isotherms and the Langmuir isotherm presents the best fit (Fig. 6). The free energy of inhibitor adsorption (ΔG^0_{ads}) was calculated by using Equation (7) as -16.4 kJ/mol from $K = 758 L.mol^{-1}$.

Surface was observed after 30 min of immersion in 0.5M H_2SO_4 solution during EN measurements in the absence and presence of inhibitor. Fig. 7a shows the SEM image of steel after immersion in blank solution which reveals a severe damage on surface due to metal pitting. Fig. 7b presents the steel surface after adding 4000 ppm inhibitor. It is observed that the surface damage has diminished in comparison to the blank solution.

The importance of sulphide inclusions as pit nucleation sites for steels is well known [23-26]. In both carbon steels and stainless steels, pits are initiated usually at MnS inclusions that their size is mainly below 5 μm [25]. Whereas in carbon steel the sulphide inclusions are more noble than the surrounding matrix which are therefore attacked preferentially, the sulphide inclusions in stainless steel, on the other hand, are usually less noble than the surrounding passive surface and are therefore selectively dissolved [24]. According to the SEM images in Fig. 7, it is possible to ascribe the EN transient waves to the pitting corrosion due to the dissolution of sulphide inclusions. In aqueous media, both chemical and electrochemical dissolution of MnS inclusions may occur. A survey of the literature indicates that a lot of attention was paid to study the electrochemical dissolution of MnS [26].

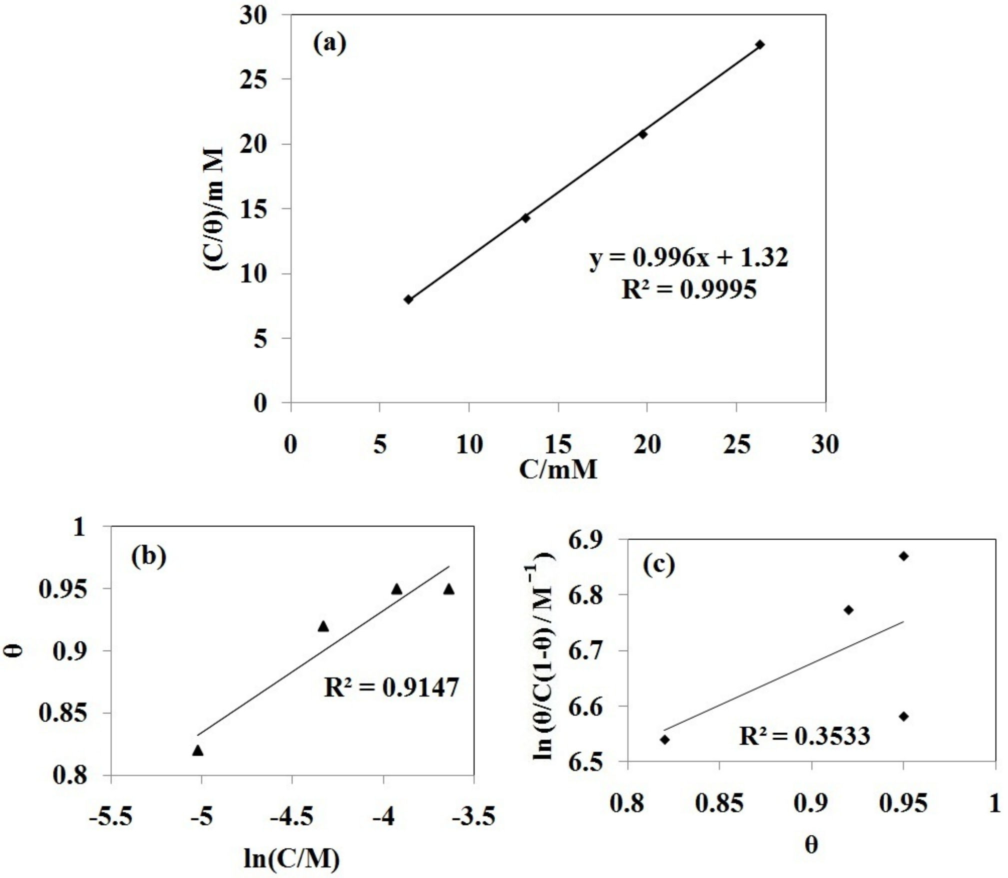

Fig. 6. Adsorption isotherms for stainless steel in 0.5M H_2SO_4 solution at the presence of different concentrations of vanillin from EN data (a) Langmuir (b) Temkin and (c) Frumkin.

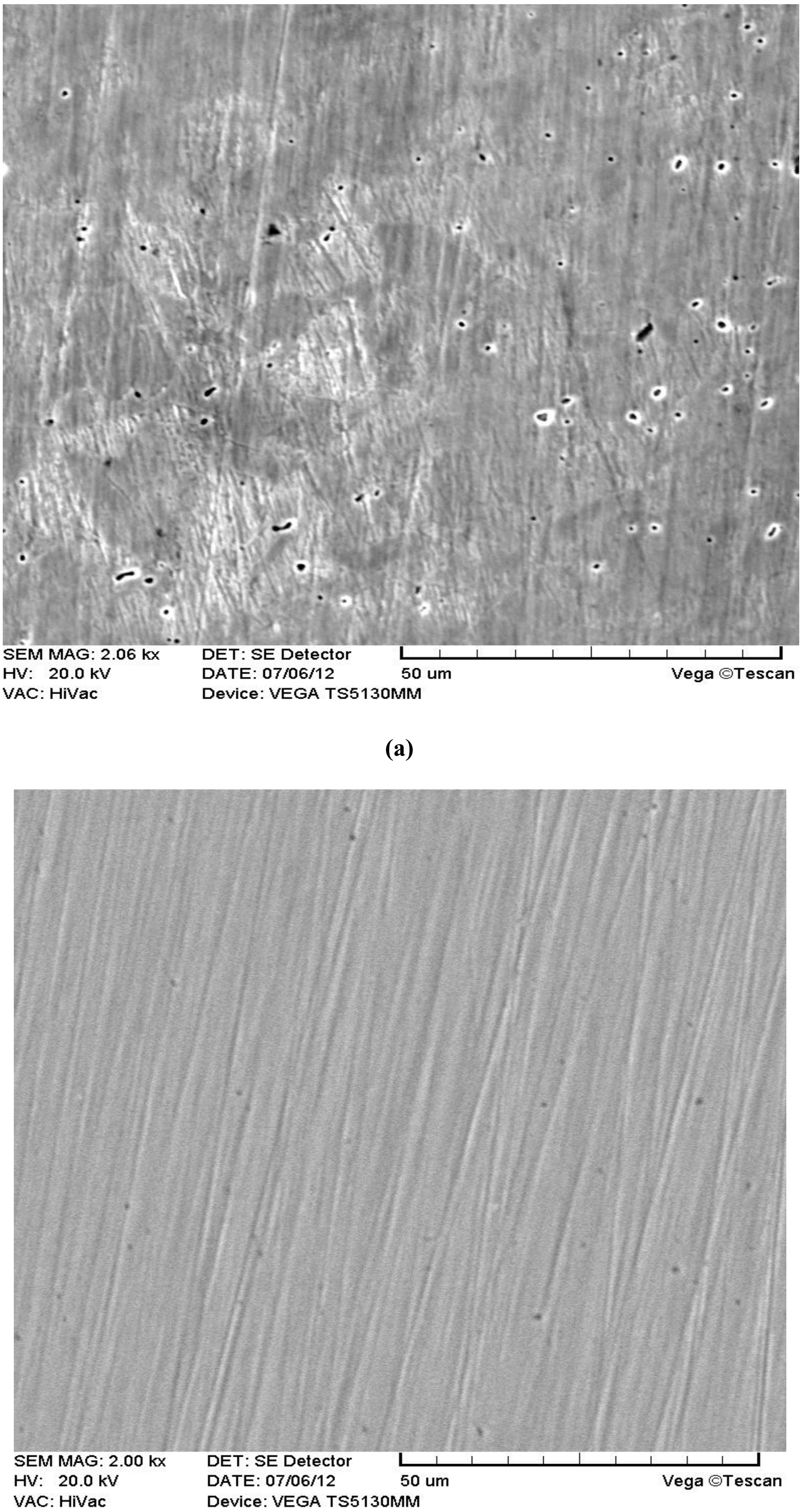

(a)

(b)

Fig. 7. SEM images of stainless steel after 30 min from immersion WEs in: (a) 0.5M H_2SO_4 solution and (b) 0.5M H_2SO_4 solution containing 4000 ppm of vanillin during EN measurements.

CONCLUSIONS

Vanillin offers interesting possibilities for corrosion inhibition because of its safe use and high solubility in water. Results obtained from potentiodynamic polarization and EIS measurements demonstrated that the adsorption of vanillin on stainless steel in 0.5M H_2SO_4 solution followed the Langmuir isotherm. The calculated values for free energy of adsorption indicated that the adsorption of vanillin on stainless steel is physical in nature.

It seems that the EN method can be applied as an alternative technique to study the corrosion behavior of inhibitors. According to calculation of the total amount of noise charges due to all PSs, it is possible to obtain the inhibition efficiency of an inhibitor. The IE values obtained from EN data for vanillin show a reasonable agreement with those obtained from potentiodynamic polarization and EIS measurements.

REFERENCES

[1] M. Sharifitabar, A. Halvaee and S. Khorshahian, Mater. Design, 32 (2011) 3854.
[2] G.M. Balamurugan, M. Duraiselvam and V. Anandakrishnan, Mater. Design, 35 (2012) 640.
[3] S.M.A. Hosseini, M. Salari and M.G. Motlagh, Corrosion, 66 (2010) 115003-1.
[4] A.S. Fouda and H.M. El-Abbasy, Corrosion, 68 (2012) 015002-1.
[5] R. Rosliza, A. Nora'aini and W.B.W. Nik, J. Appl. Electrochem., 40 (2010) 833.
[6] A.Y. El-Etre, Corros. Sci., 43 (2001) 1031.
[7] Y. Tan, Sensor Actuat. B-Chem. , 139 (2009) 688.
[8] R.A. Cottis, Corrosion, 57 (2001) 265.
[9] G. Schmitt, K. Moeller and P. Plagemann, Mater. Corros., 55 (2004) 742.
[10] G. Schmitt, Mater. Corros., 58 (2007) 924.
[11] S. Ritter, T. Dorsch and R. Kilian, Mater. Corros., 55 (2004) 781.
[12] A. Aballe, M. Bethencourt, F.J. Botana and M. Marcos, Electrochim. Acta, 44 (1999) 4805.
[13] A. Aballe, M. Bethencourt, F.J. Botana and M. Marcos, Electrochem. Commun., 1 (1999) 266.
[14] M.T. Smith and D.D. Macdonald, Corrosion, 65 (2009) 438.
[15] S.R. Allahkaram and M. Khodayari, Anti-Corros. Method. M., 55 (2008) 250.
[16] Z. Dong, X. Guo, J. Zheng and L. Xu, Electrochem. Commun., 3 (2001) 561.
[17] M. Shahidi, S.M.A. Hosseini and A.H. Jafari, Electrochim. Acta, 56 (2011) 9986.
[18] G. Achary, Y.A. Naik, S.V. Kumar, T.V. Venkatesha and B.S. Sherigara, Appl. Surf. Sci., 254 (2008) 5569.
[19] M.G. Hosseini, S.F.L. Mertens and M.R. Arshadi, Corros. Sci., 45 (2003) 1473.
[20] X. Li, S. Deng, H. Fu, G. Mu and N. Zhao, Appl. Surf. Sci., 254 (2008) 5574.
[21] M.G. Hosseini, M. Ehteshamzadeh and T. Shahrabi, Electrochim. Acta, 52 (2007) 3680.
[22] D.A. Lopez, S.N. Simison and S.R.d. Sanchez, Electrochim. Acta, 48 (2003) 845.
[23] T. Suter and H. Bohni, Electrochim. Acta, 42 (1997) 3275.
[24] G. Wranglen, Corros. Sci., 14 (1974) 331.
[25] B. Vuillemin, X. Philippe, R. Oltra, V. Vignal, L. Coudreuse, L.C. Dufour and E. Finot, Corros. Sci., 45 (2003) 1143.
[26] H. Krawiec, V. Vignal, O. Heintz and R. Oltra, Electrochim. Acta, 51 (2006) 3235.